Indian J. Res. Found., (2015) 4, 27-35. ISSN 2454-6577

INDIAN JOURNAL OF RESEARCH FOUNDATION
www.indianjournal.net

RESEARCH ARTICLE

Antibacterial activities of HAp-TiO_2 composites by Sol-Gel dip-coating technique

A. Mariappan[b], P. Pandi [a], C. Gopinathan[c], R. Rajeshwara Palanichamy[d], K. Neyvasagam[a*]

[a] *Department of Physics, The Madura College, Madurai- 625011, Tamil Nadu, India*
[b] *Madurai Institute of Engineering and Technology, Madurai- 630 611, Tamil Nadu, India*
[c] *Department of Solar energy, Madurai Kamaraj University, Madurai- 625021, Tamil Nadu, India*
[d] *Department of Physics, N.M.S.S.Vellaichamy Nadar college, Madurai- 625019., Tamil Nadu, India*

Received 6 August, 2015; Accepted 20 November 2015
Available online 10 December 2015

Abstract

The HAp/TiO_2 Composite thin films were prepared by sol-gel dip-coating technique using precursor solutions of calcium acetate and titanium (IV) isopropoxide (TTIP) employing a dipping rate of 20 seconds with different number of dipp 4, 6 and 8 respectively. The XRD analysis of HAp/TiO_2 composite has confirmed crystalline quality and the crystallite size was estimated to range from 97 nm to 116 nm. The SEM analysis reveals the formation of uniform coating with cubic structure. The presence of Ti, O, Ca and P was detected by Energy dispersive X-ray analysis. The stretching and vibrational properties of composites were reported using FTIR analysis. The surface topography, band gap analysis using AFM and UV-Vis absorption spectroscopy are also presented. The calculated energy gap values of HAp/TiO_2 composite thin films for various dipping rates are 3.854 eV,4.000 eV and 4.066 eV respectively. It has been shown that, the composite coatings depend on the number of dipping and the compositions of HAp and TiO_2. The antimicrobial activities of the HAp/TiO_2 composite thin films were investigated against *Bacillus (MTCC6428)* and *E. coli* (MTCC 739) by agar diffusion assay and REMA. These results showed that HAp/TiO_2 composite films have good bacterial adsorption and also exhibited good inhibition on positive and negative bacteria.

Keywords

Hap
TiO_2
XRD
SEM

Introduction

Hydroxyapatite (HAp) is a bioactive material having the potential and opportunity for development as bone substitutes. It is belongs to calcium phosphate class have the chemical formula is $Ca_{10}(PO_4)_6(OH)_2$ with the Ca/P stoichiometry ratio of 1.67. It has a hexagonal symmetry and unit cell lattice parameters a= 0.95nm and c=0.68nm. It has been used in biomedical applications due to have biocompatibility or non-toxity, since it is a

*Corresponding author
E-mail : srineyvas@yahoo.co.in

Published by GM SOFTWARE

main crystalline component of the mineral phase of bone and teeth [1]. In fact, it is thermodynamically stable at physiological pH and actively takes part in bone bonding, forming strong chemical bonds with surrounding bone. It is a thermally unstable compound, decomposing at temperatures from 800-1200˚C depending on its stoichiometry. In medical applications such as artificial joints, has excellent adhesion to the substrate to ensure long term fixation. It is increase the bioactivity of the implant surface due to the fact that they possess similar chemical, structural and biological properties to that of the human bone, which in stimulates osseointegration. Moreover, it is direct bond with bone since ability to induce differentiation of mesenchymal cells in to osteoblastic cells [2, 3]. HAp has some disadvantages (i) lacks the mechanical strength required for long term use in biomedical implants (Suchanek at al.1997) (ii) low melting point of phosphorous in the coating causing bioactive degradation of the coating and the use of HAp is still rather limited in load–bearing applications. In this regard many reinforcements such as alumina, zirconia, bioglass and titania have been used in HAp materials.

Among the different HAp-based composites, HAp/TiO_2 composites has attracted considerable attention, based on the combination is capable of enhancing osteoblast adhesion, inducing cell growth and provide high mechanical strength. The vital advantage of the composite coating is to increase the implants bioactivity, mechanical strength and could be applied to a photo catalytic adsorbent, especially for the removal of viruses and malignant proteins [4]. The anatase-TiO_2 is capable of oxidizing and decomposing various organisms including virus, bacteria, fungi, algae, and cancer cell [5].

Plentiful methods are offered to synthesis of HAp/TiO_2 nanostructure composite thin films such as Electro spinning process, precipitation, Micro-arc oxidation, sol-gel, spray-pyrolysis deposition (SPD), and mechanothermal process [6,7]. Among the HAp/TiO_2 composite thin films synthesis process, the sol-gel dip-coating technique is more suitable, easiest and a low cost method. In spite of this extreme experimental simplicity, by understanding the mechanism involved in the deposition having the ability to widen the range of deposition is obtained both in composition and controls the numerous of other properties.

From a thermodynamic attitude, HAp is the most stable hexagonal phase in physiological conditions, and also it is direct chemical bonding to the bone is another essential feature [8]. The main advantage of the thin film coating is to improve the implants bioactivity, mechanical strength [9]. Titania (TiO_2) is used to improve the bond strength of the HAp layer and the corrosion resistance of Ti. The corrosion resistance increases with the increasing of the TiO_2 film thickness [10].

HAp/TiO_2 composites films are papered by the sol-gel dip-coating method and are investigated by the XRD, SEM, FT-IR, EDAX and UV-Vis-NIR absorption analysis. Hydroxyapatite and anatase-TiO_2 crystalline phase is confirmed from the X-ray diffraction analysis. FTIR analysis is revealed that the presence of Ca, K, Ti, O, Na, Mg, Si, and P vibrational bands. Scanning electron microscope image is showed in the cube like shape. The roughness of the films and size of the particles are examined by AFM analysis. Band gap studies of TiO_2 and HAp are addressed by UV-Vis-NIR absorbance analysis. Bioactive nature of the HAp/TiO_2 composite films are studied against *S.aureus* and *E. coli* by agar diffusion assay and Resazurin Microtitre Assay (REMA) method.

Experimental

Preparation of HAp/TiO_2 composite thin film

Titanium(IV) isopropoxide $C_{12}H_{28}O_4Ti$ (TTIP) 97% was used as a source material for titanium (Ti) and was purchased from Sigma Aldrich. Ethanol, double distilled water and acetic acid were used as solvents and a stabilizing agent respectively. The ethanol, acetic acid and Orthophosphoric acid (H_3PO_4) were obtained from Merck. Microscopic glass slides (Borosilicate glass pk 7(2) of the dimensions 75 mm × 25 mm ×1 mm were used as substrates. The substrates were washed using soap solution for 5minutes and subsequently kept in the hot chromic acid at 40˚C for 20 minutes and then immersed in the double distilled water and acetone separately in an ultrasonic bath for 15 minutes at 40˚C.

First we prepared of HAp solution, 0.05 M solution of calcium acetate is prepared by dissolving the appropriate amount of calcium acetate Ca $(C_2H_3O_2)_2$ salt mixed with 100ml of solvent (75 ml of double distilled water and 25 ml of ethanol) and stirred for about under vigorous conditions at room temperature to obtain sol-gel solution and then 0.03 M of H_3PO_4 is added drop by drop in above prepared sol-gel solution. Finally the transparent HAp solution is formed after stirred in 5 h, while maintained the pH =10.5 of sol-gel solution by adding aqueous ammonia. The TiO_2 colloidal solution is prepared by hydrolysis of TTIP in a typical process, 1M of titanium (IV) isopropoxide is mixed with 4M of acetic acid in the same resultant solution, 10M of double distilled water and 0.1M of

HCl were mixed together and stirred vigorously for about 1h at room temperature to obtain the final transparent solution.

HAp/TiO_2 composite solution mixed together with proportion ratio of (3:1) 75 ml of HAp solution and 25 ml of TiO_2 solution is used as the film preparation for different dipping rate and different dipping cycle. Microscopic glass substrates with appropriate dimensions were dipped in the resultant sol-gel solution. Each substrate was immerse in to the solution in the dipping rate of 20 seconds, similarly dipping cycle of 4, 6 and 8 dip film is coated on substrates. Subsequently the dipped glass substrates were baked with at 100˚C for 10 minutes and then allowed to reach ambient temperature. Then the baked films were annealed at 500˚C in a muffle furnace at a constant heating rate under an air atmosphere for about 1 h.

The crystalline phase and structure of the thin film composites were determined by using Philips X'PERT-PRO powder diffractometer (XRD) (2θ=10-80˚, CuKα=1.540Å). The surface morphology and size distribution of particles was analyzed using VEGA3TESCAN. The surface compositions of the films were evaluated by Energy dispersive X-ray analysis (EDX) by BRUKER instrument. The absorption spectra of the thin film samples (4, 6 and 8 dip) were recorded in the wavelength range of 200-900nm using a Thermofischer Helios Alfa.

The vibrational properties of the HAp/TiO_2 composite thin films were analyzed by Fourier Transform Infrared Spectroscopy (FTIR) recorded by Nicolet740FTIR spectrometer in the Wave number range of 400-4000 cm^{-1}. The surface topography and the root mean square (RMS) surface roughness of prepared film (a, b, c) samples were examined by Atomic Force Microscopy (Noncontact mode, AFM, VEECO, Caliber)

Results and discussion

Structural study

Fig 1 depicts the structural phase of the HAp/TiO_2 composite thin films were analyzed by Philips X'PERT PRO powder diffractometer with Cu as the target and the Bragg reflected intensity pattern is recorded in 2θ range of 10-80° in step size of 0.05˚ as the interval. The Xray diffraction pattern of HAp/TiO_2 composites showed peak at (2θ = 31.7˚) are consistent with (211). Bragg reflection corresponds to those of a pure crystalline HAp hexagonal phase (JCPDS card No.09-432, a=9.432Å, c=6.884Å).The relatively intense diffraction peak at (2θ=31.7˚) corresponds to the (211) plane indicates a preferential orientation growth along b axis. Meanwhile XRD peak at (2θ =25.8˚) can be assigned to the crystal plane of (101) anatase TiO_2 (JCPDS card No.21-1272, a=3.785Å, c=9.513Å) and rutile phase at (2θ=66.2˚) corresponds to the plane of (221) were conform by (JCPDS card No.88-1175, a=4.517Å, c=2.940Å)

The narrow full width at half maximum (FWHM) of the tall (211) diffraction peak (β=0.071˚) leads to the largest intense calcium hydroxide used to reduces bacterial growth. Calcium hydroxide has antibacterial characteristic, enhances enzymes and growth factors release, and increases the rates of drug release [11].The crystallite size was estimated from line broadening of the diffraction lines using Scherer's equation. The prime reflections with considerable intensities such as (211), (101), (221) planes are employed for calculation of Scherer's broadening. The average crystallite size is calculated using Scherer's formula, is reported in **Table 1**.

On the other hand, the XRD analysis of HAp/TiO_2 composites the good crystallinity due to the dipping cycle at 4 predominant peaks 2θ≈31.73˚ for HAp hexagonal phase , 2θ≈ 25.29˚ for anatase nature of TiO_2 and then 2θ≈66.25˚ for the rutile phase of TiO_2 .Then the dipping cycles increases from 4 to 6 dip correspondingly 2θ shifted from 31.73˚ to 31.72˚ for HAp hexagonal phase and 2θ shifted from 66.25˚ to 66.24˚ for rutile nature of TiO_2 and the anatase phase 2θ shifted from 25.29˚ to 25.17˚ due to shifting the thickness of composites decreases and crystallinity also increases, then peak width are sharpe. It is conformed due to Full width at half maximum (FWHM) shifted β=0.087˚ to 0.071˚ for HAp hexagonal phase and FWHM β=0.087˚ to 0.09˚ corresponding rutile phase of TiO_2.

After that the dipping cycles increased from 6 to 8 dip correspondingly 2θ shifted from 31.72˚ to 31.61˚ for HAp hexagonal phase and 2θ shifted from 66.24˚ to 66.14˚ for rutile nature of TiO_2 and the anatase phase 2θ shifted from 25.17˚ to 25.01˚ due to shifting the thickness of composites decreases and crystallinity again also increases which is measured by the height of sharp peak decreased and peak will be widened, Full width at half maximum (FWHM) shifted β=0.071˚ to 0.092˚ for HAp hexagonal phase and FWHM β=0.09˚ to 0.10˚ corresponding rutile phase of TiO_2. It is concluded that the peak shifts is reflected by a change in lattice parameters of apatite structures and also the precursors ratio (75% HAp: 25% TiO_2) is used for composite

preparation, to decrease size of crystalline gradually as shown in table(1) due to the increase the TiO_2 precursor content on substrate coating by increasing dipping rate. It is also showed that at 8 dip of anatase phase peak intensity is highest, compared to rutile phase peak intensity. The peak shifts and TiO_2 concentration is one of the reason for reduce the grain size, while increasing the dipping rate [6].

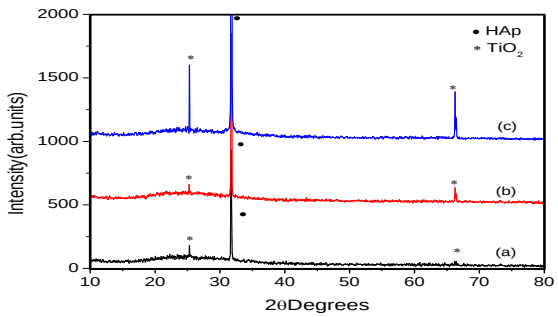

Fig 1 XRD pattern of the composite films: (a) 4dip, (b) 6 dip, (c) 8dip.

Table 1 Grain size of HAp/TiO_2 composite film for various dipping rate.

Film Samples	(Average grain size in nm)
4dip	116
6dip	107
8dip	97

SEM

The surface morphology and the microstructure of the HAp/TiO_2 composites were analyzed using Scanning Electron Microscope of model VEGA3 TESCAN. During the reaction, the orientation, size and shape of the HAp/TiO_2 composites mainly depends on the growth time, growth temperature, substrate, reactant concentration, and acidity [4]. It reveals that under in situ preparation conditions, hydroxyapatite is stable and keeps its cube like morphology while Ti-complex is easily hydrolyzed, then nucleated, grown as anatase elongated plate like crystals in the HAp/TiO_2 composites . Initially increase the dipping rate 4 to 6 dip, to increase the amount of titania, leading to increase the formation of anatase crystals, so that thin elongated plate-shaped are derived. The microstructure shows the small cube like structure, which is much useful for biomedical applications because it allows cell adhesion, vascularization and nutrition flow.

After increasing the dipping rate from 6 to 8 dip due to increase of titania, effect of anatase crystals on the HAp/TiO_2 composites morphology may be considerably as small and their morphology is like cube structure (like HAp crystals). It could be observed that, increasing the dipping rate gradually increase titania concentration reduce the size of the HAp particles in the composite coating. Our results are well agreed with already reported value [6].

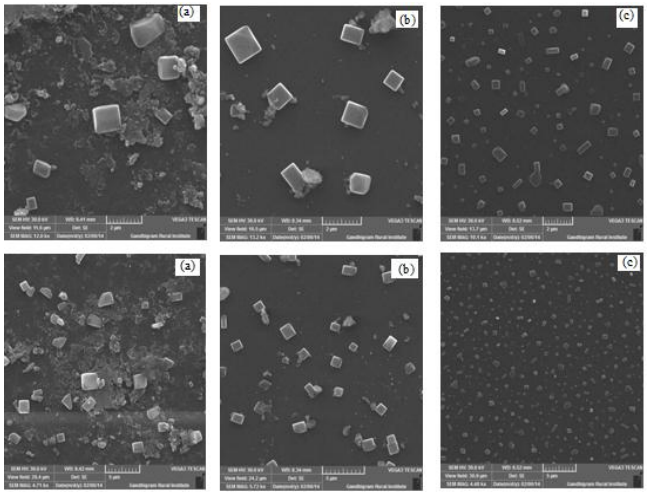

Fig 2 SEM image of HAp/TiO_2 composite thin films a) 4dip, b) 6 dip and c) 8dip

EDAX

An energy dispersive X-ray spectroscopy (EDX) analysis recorded during the SEM analysis which gives on information about the elemental composition. The EDX spectrum was collected with an accelerating voltage and a working distance of 30 Kv and 14.9mm respectively. **Fig 3** depicts EDX spectrum of the top portion of a HAp/TiO_2 composite thin film at dipping cycle is 6 samples. Here, we have collected the EDX spectrum from the top view of composite film by using fast moving electrons X-ray signals.

The Oxygen peak at 0.5Kev (O kα) reveals that the O is dominant peak compare to the peaks corresponds to Ca and Ti. The Ca peak collected between≈ 0.3 to 0.4kev (Ca kα), P peak collected at 2.01kev and the Ti peaks at 0.4 to 0.44Kev, 4.5kev (Ti k_α) and 4.9 kev (Ti k_β) are observed in signals coming from top portions of the sample. The HAp/TiO_2 composite film grown on the dip coated layer have Ca, Ti, Si, Na and O ratios in the top portion of the sample of 2.52:1.90:20.52:8.93:63.50 at,% respectively. The EDX analysis clearly revealed that presents of main elements of the composites are Ca, P, Ti and O.

This result is a good agreement with the literature value [11, 14]. In addition characteristic, elements present on K, Na, Si, Mg energy peaks are appeared at ≈ (0.3 to 3.26, 1.03, 1.76, 1.23 kev respectively.

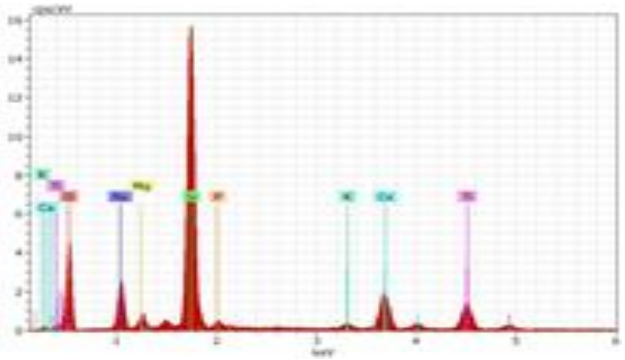

Fig 3 EDAX profile of 6dip. HAp/TiO_2 composite thin film

Optical studies

Semiconductors such as metal oxides have both ionic and covalent bonds between atoms, which gives rise to an energy band gap in the materials, from the absorption spectrum of semiconductors is directly determine the electronic structure of the material by exciting electrons from the valence band to the conduction band using ultraviolet and visible radiation. Hence, UV-Vis photons were passed through the HAp/TiO_2 composite and recorded in the wavelength range of 190-1000 nm [15,16].

The optical absorbance spectra of the HAp/TiO_2 composite thin films in the range of 250-400nm are shown in Fig 4. From the Fig 4, it is clear that the strong response in the UV region (200-400 nm).A method for probing the band structure of semiconductors is to be measure the optical absorption. In the absorption process, a photon of known energy excites an electron from a lower to a higher energy state. For determination of the fundamental gap, band-to-band transitions are probed. However, because the transitions are subject to selection rules, the determination of the energy gap from the "absorption edge" of the luminescence peak is not a straight forward process. Because the momentum of a photon is very small compared to the crystal momentum, the optical process should conserve the momentum of the electron. In a direct-gap semiconductor, momentum-conserving transition connects states having the same k-values. In an indirect band gap, semiconductor momentum is conserved via a phonon interaction. Although a broad spectrum of phonons is available, only those with the required momentum change are usable. These are usually longitudinal and the transverse-acoustic phonons. In addition, the indirect process is a two-step event. Therefore, indirect optical processes have very low transition probabilities. In this study HAp/TiO_2 composite thin film possesses an direct band system and the band gap energies of the HAp/TiO_2 composite thin film were calculated using the Taue's plot $E_g=(\alpha h\gamma)^2/(h\gamma)$ method **Fig 4**. Where $h\gamma$, α and E_g are the photon energy, absorption coefficient and band-gap of the inter-band transition respectively.

The calculated energy gap values of HAp/TiO_2 composite thin films for various dipping rates are 3.8,4.0 and 4.09ev respectively, while that of HAP pure was 5.0 ,5.5and 5.41ev respectively . From the calculated values reveals that increase the dipping rate gradually the band gap value also increases. It is good agreement with energy gap of pure HAp was 5.3 ev which is in the range of 4.5-5.4ev and composites of film HAp/TiO_2 is ≈3.6 ev and reported in the previous studies [17- 20].

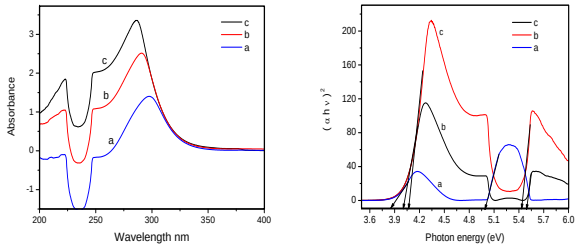

Fig 4 UV-Vis-NIR adsorption spectra of HAp/TiO_2 composites thin films for a) 4, b) 6 and c) 8 dip

FTIR

Fig 5 illustrates the complementary information in the presence of HAp and TiO_2, FT-IR analysis is observed on 4, 6 and 8 dips of HAp/TiO_2 composite thin films in the spectral region of 400 to 4000 cm^{-1}.

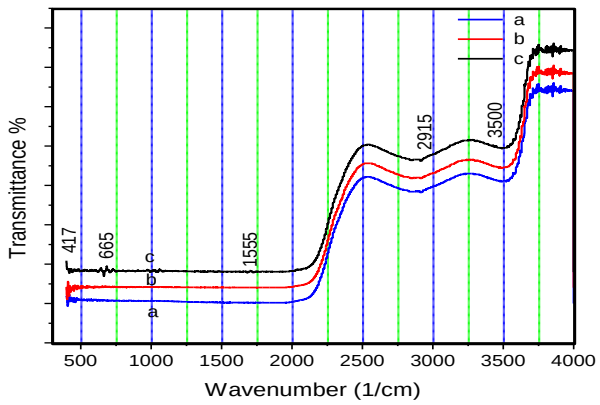

Fig 5 FTIR Analysis of HAp/TiO_2 composite thin films a) 4 dip. b) 6 dip and c) 8 dip.

The characteristic absorption peaks of phosphate groups belong to 472 - 567 cm^{-1}. For the OH^- group of HAp, peak positions are 636 - 3575 cm^{-1}. The bending mode of H_2O bond at 1648 cm^{-1} as well as its stretching mode in the range of 3000–3700 cm^{-1}, which is almost overlapped by the O–H vibration mode of HAp at 3570 cm^{-1}, are observed in the FT-IR analysis of the HAp-TiO_2 composite thin films. The TiO_2 characteristic vibrational peaks at 550 and 700 cm^{-1} are bonded Ti–O [22].

Atomic Force Microscopy

AFM analysis is used to characterize the surface morphologies of the HAp/TiO_2 composites films **Fig 6a** image shows that surface topography is almost non-uniform throughout the surface and the thickness appears somehow more non-homogeneous for this film. When scanning areas to 2.5-2.5 μm^2, the film is observed to present well-defined grain boundaries. Although the grain boundaries are mostly cubic narrow particles. The surface roughness is around 84.4 nm.

Fig 6b Image shows the surface roughness of the composite film is decreased, while further increasing the dipping rate. The size of particle is also reduced further when increasing dipping rate from 4 to 6 dip composite films. The grain boundaries are clearly seen on scanning area in 2.5-2.5 μm^2. The area roughness R_a (average height above the centre line) and the area R_{rms} (root mean square of R_a) is calculated and presented in **Table 3** [21].

Fig 6c Image shows the uniformity of the film is increased after increasing the dipping rate. The size of particle is also reduced further when increasing dipping rate from 6 to 8 dip composite films. It is shows the relevant changes in the surface topography recorded on a 10-10μm^2 area of HAp/TiO_2 composite coating. The uniformity of the coating was further increased due to increasing the dipping rates. The grain boundaries are clearly seen on reducing the scanning area for 2.5-2.5 μm^2. The area roughness R_a (average height above the centre line) and the area R_{rms} (root mean square of R_a) value is calculated and presented in **Table 3**. The depth profile analysis also gives information about the surface topography. There is a single horizontal line are randomly chosen to analyze the uniformity of the composite thin films (4, 6 , 8 dip). In the 4 dip composite film the profile changes non-uniformly. So the line profile height various simultaneously. There is further improvement in the profile for 6 dip composite film and it conforms the increase in the film growth are gradually by increasing dipping rate. In 8 dip composite film the profile shows very uniform pattern for all area. It is concluded that, the increase in the dipping rate gradually induce the uniform growth of the structure and reduces the size of the particle which is also well clear from SEM analysis and XRD analysis.

Table 2 Roughness values (average height above centre line) R_a and R_{rms}(root mean square of R_a)of the HAp/TiO_2 the composite films.

Sample	R_a (average height above centre line) (nm)	R_{rms} (root mean square of R_a) (nm)
4dip	57.307	84.428
6dip	13.732	20.583
8dip	7.948	12.593

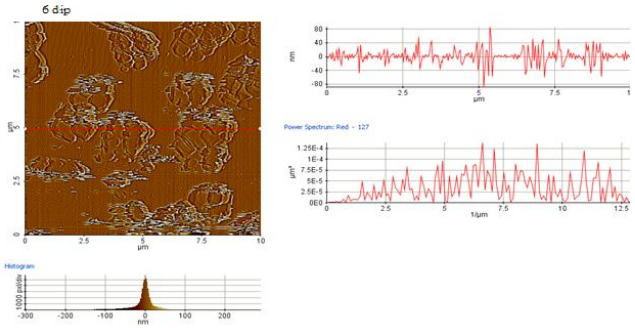

Fig 6 b) The horizontal line profile of HAp/TiO_2 composite thin films (b) 6 dip.

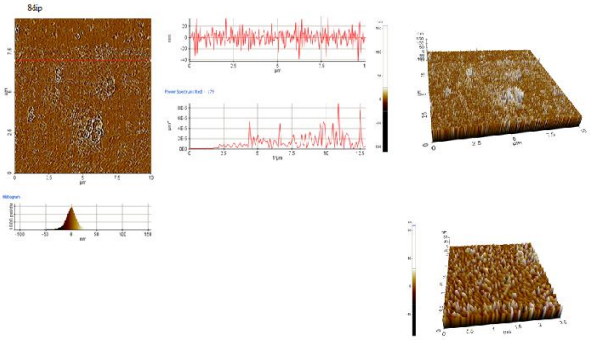

Fig 6 c) The horizontal line profile of HAp/TiO_2 composite thin films (c) 8 dip.

Antimicrobial activity

The photographs of the antimicrobial activity of the HAp/TiO_2 composites thin films are investigated against *S. aureus* (MTCC 1430) followed by E-*coli* (MTCC 739) by agar diffusion assay and Resazurin Microtitre Assay (REMA) (Sarker and Nahar2007) [23]. Since *S. aureus* and the *Escherichia coli* have been implies to be the important common pathogens in biomaterial-associated infections [28].

However, there are some differences between gram positive *S.aureus* and gram negative *E. Coli*. *S. aureus* has slightly less bacterial activities in growth curves, protein leakage, and

inactivation of LDH (Lactate Dehydrogenase activity) than E. coli's. The morphological destruction of bacterial cell of *S. aureus* was weak than *E. coli*. This difference was possibly attributable to the difference of the peptidoglycan layer of the bacterial cell between gram positive *S. aureus* and *E. coli*, an essential function of the peptidoglycan layer is to protect against antibacterial agents such as antibiotics, toxins, chemicals, and cell memberane [24].

The combinations of HAp and TiO_2 composites with different dipping rate (4 dip, 6 dip and 8 dip) for various TiO_2 concentrations is important factor for antimicrobial activity. Hence with increasing the dipping rate due to decrease the TiO_2 concentration has the factor for antimicrobial activity.

Initially lower dipping rate (4 dip) sample at higher concentration of the TiO_2 in the composite, it can be used as an antimicrobial material or coatings in various day to day applications (bath room tiles, doorknobs, packing materials etc.) by controlling the spread of disease causing microbes. Since HAp has the good adsorption property and TiO_2 is well known for its photo-degradation nature the composites can be used as absorbent and degradation agent for the pollutants. Hence the combination HAp and TiO_2 has excellent applications in biomedical, antimicrobial and environmental friendly applications [27].

In case of (8 dip) highest dipping rate of sample clearly implies that the bacterial growth decreases and exponentially with increasing dipping rate increases the HAp concentrations (TiO_2 concentration decreases) up to certain concentration. In such a case, basically E. *coli* has a relatively thin cell wall made of peptidoglycans and lipopolysaccharide [27]. It is concluded that increasing the dipping rate due to increase the HAp concentration (decrease the TiO_2 concentration) change of inhibited area of zone also increases due to change antimicrobial activity of against *S. aureus* (MTCC 1430) followed by E. *coli* (MTCC 739) by agar diffusion assay and Resazurin Microtitre Assay (REMA).

The initial concentration of the microorganisms used was 1×10^8 cells/ml (test culture).The agar diffusion assay is performed on Mueller–Hinter (MH) agar. 1 % test culture is seeded into the medium before pouring it in to Sterile Petri plates to form a layer of 4 mm thickness. 4 , 6 and 8dip composite film are loaded on sterile discs (Himedia). Which are placed on the MH agar plates and incubated for 24 h at 37 °C. The results are recorded by observing the zone of inhibition as shown in **Table 3** [24-30].

It is good agreement with reported that S. aureus has exhibited the most susceptibility to the composites in comparision with E. Coli. [25]. The gram-positive bacteria have a relatively thick wall composed of many layers of peptidoglycan polymer, and only one membrane (plasma membrane). The gram-negative bacteria have only a thin layer of peptidoglycan and a more complex cell wall with two cell membranes, an outer membrane, and a plasma membrane. The addition of the outer membrane of the gram-negative bacteria cells influences the permeability of many molecules. Under certain conditions, the gram-negative bacteria are more resistant to many chemical agents than gram-positive cells [27]. The antibacterial activity of the HAp/TiO_2 composites on *E.Coli* and *S.aureus* can be seen in **Fig 6** [31, 32].

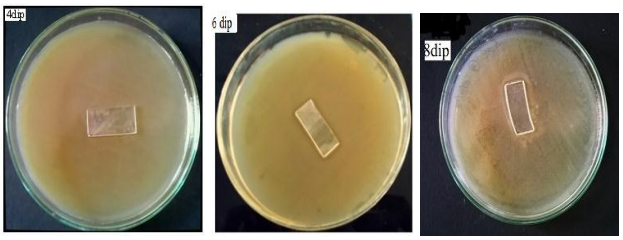

Fig 7 shows antimicrobial activities of the HAp/TiO_2 thin films were investigated against *E. coli* (MTCC 739)

Fig 8 shows antimicrobial activities of the HAp/TiO_2 thin films were investigated against *S. aureus* (MTCC 1430)

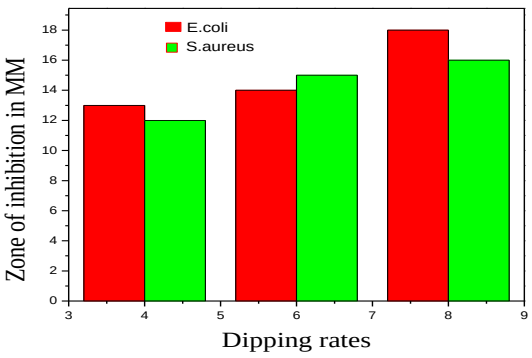

Fig 9 Antimicrobial activities of the HAp/TiO_2 thin films were investigated against *E. coli* and *S. aureus*

Table 3 Antimicrobial activities of the HAp/TiO_2 thin films were investigated against *E. coli* (MTCC 739) and *S. aureus* (MTCC 1430)

Sample No	Zone of inhibition in mm	
	E.coli	*S.aureus*
4	13	12
6	14	15
8	18	16

Conclusions

HAp/TiO_2 composite was prepared by simple sol-gel dip-coating method. The XRD analysis gives the good crystalline nature of HAp/TiO_2 composite film. The micrographs confirm that the prepared HAp/TiO_2 composite films are in the cubic like structure form. Also it shows that, various dipping rates of prepared composite were shows that the change of morphology considerably and EDAX confirm the presence of elements in the composite. From the AFM analysis we observed that the increase in the dipping rate gradually induces the uniform growth of the composite film and reduces the size of the particle. The presences of vibrational bands are observed from the FTIR analysis. The optical studies of HAp/TiO_2 composite are gives the energy gap of HAp/TiO_2 by absorbance spectra of composites. The antimicrobial effect shows good inhibition on two types of bacteria *S. aureus* and *E. coli* even under atmospheric conditions.

References

[1] J.H. Lee, II T. Kim, R. Tannenbaum, M.L. Shofner, (2012), J.Mat.Chem., 22, (2012), 11556.

[2] L. Mohan, D. Durgalakshmi, M. Geetha, T.S.N. Sankaranarayanan, R. Asokamani, *Ceramics Inter.*, 38, (2012), 3435.

[3] A.F. Sheikh, A.M. Kanjwal, H. Yong Kim, H. Kim, *Appl. Surf. Sci.*, 257, (2010), 296.
M. Enayati-Jazi, M. Solati-hashjin, A. Nemati,

[4] F. Bakhshi, *Microstruct.*, 51, (2012), 877.

[5] H. Chen, C. Chung, T. Yang, C. Tang, J. He, *Appl. Surf. Sci.* 266, (2013), 73.

[6] A.J. Nathanael, D. Mangalaraj, N. Ponpandian, *Composites Sci. Tech.*, 70, (2010), 1645.

[7] A. Nakajima, K. Takakuwa, Y. Kamashima, M. Hagiwara, S. Sato, Y. Yamamoto, N. Yoshida, T. Watanabe, K. Okada, J. Photochem. Photobiol. A Chem., 177, (2006), 94.

[8] A. Fahami, B. Nasiri-tabrizi, J. Adv. Cer., 2(1), (2013), 63.

[9] A. J. Nathanael, N.S. Arul, N. Ponpandian, D. Mangalaraj, P. Chen, Thin Solid Films, 518, (2010), 7333.

[10] M. Ansari, S.M. Naghib, F. Moztarzadeh, A. Salati, Ceramics-SiliKaty, 55(2), (2011), 123.

[11] S. Pezelj-Ribarie, I. Brekalo, I. Miletie, M. Abram, Z. Karlovie, I. Anie, Acta Stomat. Croat., (2001), 475.

[12] B. Liu, E. S. Aydil, J. Am. Chem. Soc. 131, (2012), 3985.

[13] C. Angeles-Chavez, J. Antonio, T. Antonio, M.A. Cortes-Jacome, Chemical quantification of Mo-S,W-Si and Ti-V by Energy dispersive Xray spectroscopy, 978-953-307-967-7.

[14] K. Sattler, The energy gap of clusters nanoparticles, and Quantum dots, Handbook of thin films Materials and Magnetic Thin films. Edited by H.S.Nalwa copy right@2002 by academic press, ISBN 0-12-512913-0.

[15] P. Sondarrajan, K. Sankarasubramanian, K. Sethuraman, K. Ramamurthi, Cryst. Eng. Comm.,16 (2014) 8756.

[16] K. Matsunaga, A. Kuwabara, Phys. Rev. B, 75, (2007), 1.

[17] M. Ardyanian, M.M. Bagheri-Mohagheghi, N. Sedigh, Indian Academy Sci., 78, (2012), 625.

[18] S. Baskoutas, A.F.Terzis, ,J. Appl. Phys., 99, (2006), 013708.

[19] R. Vijayalakshmi, V. Rajendran, Archives Appl. Sci. Res., 4(2), (2012), 1183.

[20] A.J. Nathanael, D. Mangalaraj, P, C. Chen, N. Ponpandian, Comp. Sci. Technol., 70, (2010), 419.

[21] M. Raposo, Q. Ferreira, P.A. Ribeiro, A Guide for Atomic force microscopy analysis of soft condensed Matter," Modern research and educational topics in microscopy, A.Mendez-vilas and J. Diaz(Eds.) FORMATEX (2007).

[22] H.U. Lee, Y.S. Jeong, S.Y. Park, S.Y. Jeong, H. G. Kim, C.R. Cho, *Current Appl. Phy.*, 9(9), (2009), 528.

[23] D. Satyajit, Sarker, L. Nahar, Y. Kumarasamy, Methods, 42, (2007), 321.

[24] Kim, S. Hwan, H.-Seonlee, D. Seon Ryu, S. Jae Choi, D. Seok Lee, *J. Microbial, Biotechnol.*, 39(1), (2011), 77.

[25] A.W. Hill, A.L. Shears, K. G.Hibbitt, , Amer. Soc. Microbiology, 14, (1976), 257.

[26] G. Fu, P.S.Vary, C. Tsu Lin, J. Phys. Che. B,109,(2005), 8889.

[27] A.J. Nathanael, J.H. Lee, D. Mangalaraj, S.I. Hong, Y.H. Rhee, Powder Tech., 228, (2012), 410.

[28] H.S. Ragab, F.A. Ibrahim, F. Abdallah, A. Al-Ghamdi, F. El-Tantawy, F. Yakuphanoglu, *J. Pharm. and Biol. Science*, 9(1), (2014), 77.

[29] L. Juan, Z. Zhimin, M. Anchun, Lilei, Z. Jingchao, *Inter. J. Nanomedicine*, 5, (2010), 261.

[30] N. Ma, X. Fan, X. Quan, Y. Zhang, *J. Membrane Sci.*, 336, (2009), 109.

[31] C.S. Ciobanu, S.L. Lconaru, P. Le Cousumer, L. Violeta Constantin, D. Predoi, *Nanoscale Res. Lett.*, 3 ,(2012), 324.

[32] U.G. Akpan, B.H. Hameed, *Appl.Catal. A*, 375, (2010), 1.